Journal of Structural Chemistry. Vol. 57, No. 7, pp. 1348-1354, 2016.

THEORETICAL AND EXPERIMENTAL STUDY OF MONONUCLEAR Cu(II) ACETATE-BIPYRIDINE COMPLEX

M. A. Kremennaya, M. A. Soldatov, A. P. Budnyk, T. A. Lastovina, and A. V. Soldatov

UDC 544.144.22:544.182.32:544.182.36

Cu(II) acetate-bipyridine complex has been synthesized. A series of experimental and theoretical spectroscopic studies was carried out for the freshly prepared sample. The local atomic and electronic structure was theoretically analyzed based on functional density theory and the structural models of the complex was obtained for various solvents. IR and XANES spectra were experimentally measured and modelled in the framework of functional density theory in a generalized gradient approximation to provide information on the chemical bond and local surroundings of copper. The powder X-ray pattern of the Cu(II) complex was obtained. The measured ESR spectra of the acetate-bipyridine complex at room temperature for the solid sample and solution in DMF confirms the formation of the mononuclear square planar complex.

DOI: 10.1134/S0022476616070076

Keywords: Cu(II) acetate-bipyridine complex, precursor of copper oxide nanoparticles, IR spectra, XANES, ESR, density functional theory, local atomic and electronic structure.

INTRODUCTION

Coordination compounds of transition metal salts with bidentate chelate ligands are important complexes for structural studies in coordination chemistry with the wide sphere of possible applications from catalysis [1, 2] to bioorganic chemistry [3]. Carboxylate complexes are the most investigated ones. So in the works [4, 5] two carboxylate metal complexes, binuclear of the paddle wheel type and basic triangular trinuclear, were studied. B. Ye et al. [6] report structural studies of mono-, bi- and trinuclear complexes formed in the result of the reaction between acetates of divalent metals with 2,2′-bipyridine (bpy) in methanol to elucidate the geometry of the metal ions presented in metalloenzymes. Mononuclear complexes were formed by the addition of a perchlorate ion in the reaction solution. Based on literature data for the synthesis of trinuclear acetate complexes of Fe(II) and Mn(II), B. K. Koo attempted the synthesis of the similar Cu(II) complex, however, a mononuclear complex has been obtained eventually [7]. Using single crystal X-ray diffraction he determined the structure of $[Cu(O_2CMe)_2(bpy)]$ complex and established its square-planar geometry (where bpy is 2,2′-bipyridine; Me is methyl group) which belongs to the triclinic crystal system.

Anew metal complexes with carboxylate and nitrogen containing ligands were the subject of the increased interest because of its biochemical properties [8]. In particular, Cu(II) containing complexes show high antibacterial, antifungal and

International Research Center “Smart Materials”, Southern Federal University, Rostov-on-Don, Russia; kremennayamariya@gmail.com. Translated from *Zhurnal Strukturnoi Khimii*, Vol. 57, No. 7, pp. 1423-1429, September-October, 2016. Original article submitted November 20, 2015.

anticancer activity [9] and even cisplatine was proposed as a promising alternative of the preparation [10]. Besides, the effect of metal complexes is considered more effective in action than free ligands [11]. The oxidation or thermal decomposition of various copper complexes can serve as a promising technique for the preparation of copper and copper oxide nanoparticles [12]. In addition, they are of interest in creation of magnetic storage cells, photoelectric [13] and biological systems [14]. In the case of liquid phase synthesis, bipyridine can operate as a surface-active compound that assists in controlling shape, size and purity of the particles obtained [15].

From these reasoning we repeated the synthesis of $[Cu(O_2CMe)_2(bpy)]$ compound and performed a series of experimental and theoretical works. In order to span the gaps in our knowledge on the complex, we used X-ray absorption spectroscopy and electron paramagnetic resonance spectroscopy to yield extended information on the copper center in the molecule. IR spectroscopy shows the presence of organic ligands in the complex, which are difficult to find in the literature, also they are observed in the powder X-ray diffraction pattern that will be reported below.

At present, density functional theory (DFT) is the most-used quantum chemical method for the study of 3*d* metal complexes with aromatic organic ligands [16-22]. BP [23] and B3LYP [24, 25] exchange-correlation potentials were used to perform the geometrical optimization of the molecular structure of the complexes under study.

The application of B3LYP hybrid exchange-correlation potential is the most precise and effective method of quantum chemical calculations for coordination compounds, in particular, for biological metal-containing complexes [16-22, 26-28]. BP functional is also used for the study these complexes [17, 29-31] as a good trade-off between the desired accuracy and computational resources. In this work, the choice of the exchange-correlation functional is based on the comparison between the results of the molecular structure optimization and crystallographic data. Further for the optimized structures the theoretical spectra of X-ray absorption and IR profiles were calculated. As far as is known, similar data for $[Cu(O_2CMe)_2(bpy)]$ complex have not been reported so far.

EXPERIMENTAL

Synthesis. Synthesis technique was taken from [7] and slightly modified. $Cu(CH_3COO)_2{\cdot}H_2O$ (0.81 g) was dissolved in 20 ml of dymethylformamide (DMF) and agitated by a magnetic stirrer to the complete dissolution. Then the solution of 2,2′-bipyridine (0.43 g) in 10 ml of DMF was added. The solution was mixed for 8 h at room temperature. We separated a light-blue deposition by sedimentation and washed with ethyl ether. The powder obtained was dried in a vacuum oven at 60°C. All reagents had CP grade and did not undergo an additional purification.

Characterization. The X-ray powder diffraction profile (XRPD) was obtained on a Ultima IV powder diffractometer (Rigaku) using CuK_α radiation (λ = 1.5406 Å). The operating voltage and current were 40 kV and 40 mA, correspondingly. The profile was recorded using the scanning step 0.02° and exposition time 2 s. X-ray Absorption Near Edge Structure spectra (XANES) were measured in transmission mode on a laboratory X-ray absorption spectrometer R-XAS Looper (Rigaku) using a scintillation detector SC-70. A crystal-monochromator Ge(311) was applied to obtain better statistics with the acceptable resolution 3.2 eV. The measurements were carried out using exposition time 90 s per point with the operating condition of the device 18 kV and 80 mA. IR Fourier spectra were measured on a Vertex 70 (Bruker) spectrometer with the resolution 2 cm^{-1} using a diamond attachment of total internal reflection Platinum ATP. Electron spin resonance spectra (ESR) were obtained on an EMX plus (Bruker) spectrometer using 9.65 GGz frequency and 100 kGz modulation.

DFT calculations were performed using software package ADF2014.05 [8-10]. The adapted model of the Cu(II) acetate-bipyridine complex was built using a standard instrument Structure Tool, and manifests a plane molecule consisting of a copper atom coordinated by one bipyridine and two acetate ligands (Fig. 1).The refinement of the structure was performed by the minimization of the total energy of the system. The geometry optimization was performed using BP and B3LYP exchange-correlation potentials and DZ (DoubleZ) basis set. The best agreement with experimental data was achieved at the total system charge 2 and total spin 1. The several cases of the molecular environment were studied: vacuum, water and ethanol. Accounting of molecular surroundings of water and ethanol was performed using COSMO solvent.

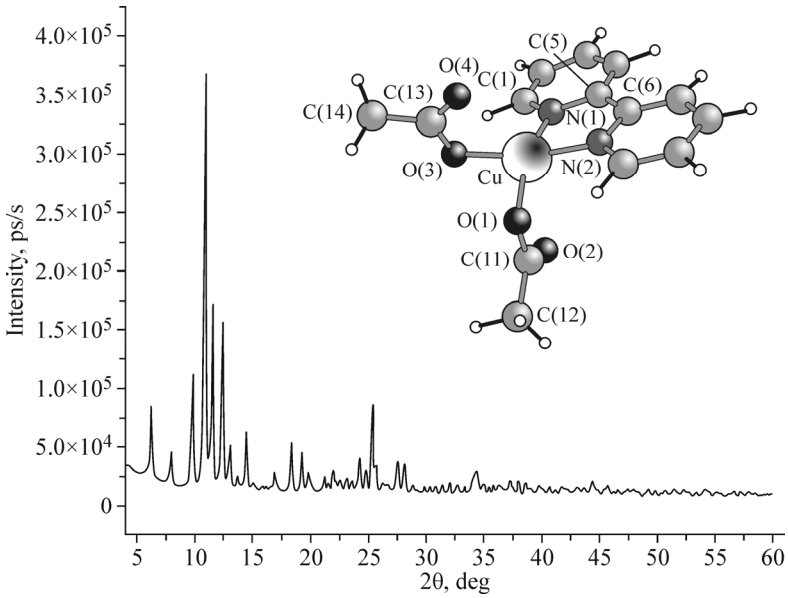

Fig 1. X-ray diffraction pattern of $[Cu(O_2CMe)_2(bpy)]$. Inset shows model structure of the Cu(II) acetate-bipyridine complex.

The calculation of theoretical IR spectra was analytically performed using ADF2014.05 software package after the geometry optimization procedure. The analytical frequencies were calculated using Kohn–Sham perturbation equations [35-37] using PBE [38] exchange-correlation potential because the calculation of the analytical frequencies has restrictions in the application of exchange-correlation potentials. The given limitation is related to the features of the obtaining of derivative formulas.

The calculations of theoretical XANES spectra were carried out using the accelerated version of FDMNES software package [39, 40]. The spectra of X-ray absorption above the Cu*K* edge were calculated by the finite difference method in the total potential of the system. The calculations were conducted for the grid of $R = 5.5$ Å radius in the increments of 0.25 Å and include 33 atoms.

RESULTS AND DISCUSSION

The powder diffraction experimental profile of the freshly prepared sample is presented in Fig. 1. This profile of the complex does not presented in the literature before because the crystallographic study of the new material was performed using a single crystal.

The insert of Fig. 1 shows the coordination geometry of $[Cu(O_2CMe)_2(bpy)]$ complex that corresponds to a monomeric square-planar structure with bipyridine and two acetate ligands. For optimization of the molecular structure two BP and B3LYP exchange-correlation potentials are used. Table 1 presents the selected values of the bond lengths and angles in comparison to the crystallographic data from [7]. From the comparison of the values in Table 1, we conclude that both functionals provide good agreement with the crystallographic data. Nevertheless, the mean deviation of the bond length for BP is 0.06 Å and for B3LYP is 0.7 Å, and the mean deviation of the angles for BP is 4.6° and for B3LYP is 4.2°. Because BP exchange-correlation potential requires less computing costs, this potential was used for the calculation of the geometrical parameters of the molecule in different solvents. The results are also presented in Table 1. On addition of the solvents (water and ethanol), the general tendency was observed for both the models: acetate ligands rotated relative to the plane part of the molecule (the plane of copper and bipyridine) with the angle decreasing and also the bond lengths between the metal center and ligands decrease.

Fig. 2 presents the isosurfaces of the electronic density for the highest occupied molecular orbital (HOMO) and the lowest occupied molecular orbital (LUMO). HOMO is localized on the 2.2′-bipyridine ligand that is rather typical for

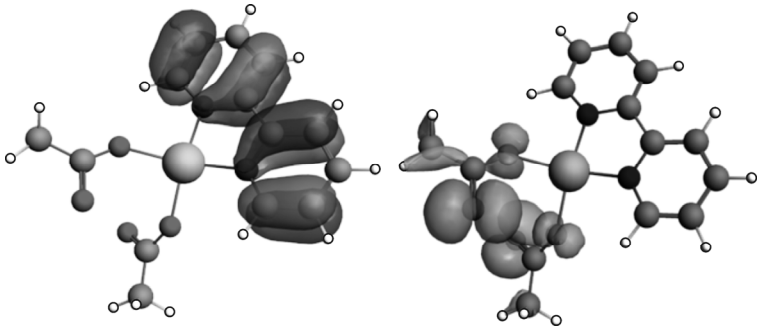

Fig. 2. Isosurfaces images of the electron density for HOMO (left) and LUMO (right) in $[Cu(O_2CMe)_2(bpy)]$.

TABLE 1. Comparison between Selected Bond Lengths (Å) and Angles (deg) for Models Calculated Using Exchange-Correlation Potentials BP and B3LYP and Crystallographic Data (XRD) Obtained in [7]

Bond length Angle	XRD [7]	B3LYP	BP	BP Cosmo:H_2O	BP Cosmo:Ethanol
Cu–O(1)	1.927(4)	2.030	1.966	1.906	1.925
Cu–O(3)	1.952(4)	2.032	1.967	1.909	1.930
Cu–N(1)	2.020(5)	1.973	1.945	1.922	1.953
Cu–N(2)	2.015(5)	1.975	1.942	1.924	1.953
O(1)–Cu–O(3)	90.5(2)	93.1	91.1	90.4	90.6
O(1)–Cu–N(1)	173.0(2)	165.9	167.2	175.4	176.4
O(1)–Cu–N(2)	96.3(2)	94.5	94.2	93.0	93.4
O(3)–Cu–N(1)	93.2(2)	93.6	93.6	92.8	93.6
O(3)–Cu–N(2)	172.9(2)	161.5	167.1	174.5	174.0
N(1)–Cu–N(2)	79.8(2)	82.8	83.8	84.0	83.2

Cu(bpy) complexes [41]. LUMO spreads around oxygen atoms possessed by two acetate ligands and the *d* orbital of copper. The dipole moments of the complex is $96.4 \cdot 10^{-30}$ C·m (28.9 D) and it infers that the complex is polar and prone to a reaction with other charged compounds [42].

Fig. 3*a* shows the experimental XANES spectrum. Its profile has a typical shape and the position of the main maximum at 8997 eV for Cu(II)-containing complexes [12], whereas Cu(I)-containing complexes are characterized by the presence of the pre-edge feature at the energy 8984 eV. Fig. 3*a* shows the theoretical XANES spectra calculated using BP

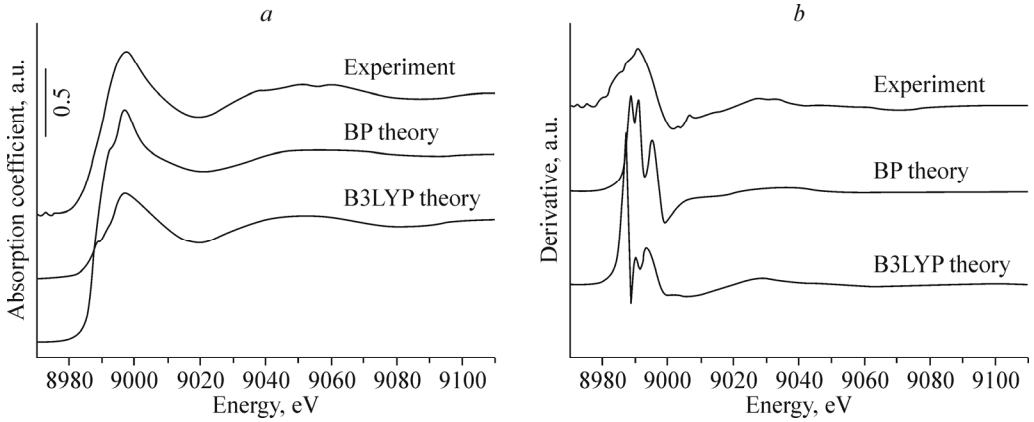

Fig. 3. Normalized experimental Cu*K* XANES spectrum of synthesized Cu(II) acetate-bipyridine complex and theoretical XANES spectra for the models obtained using BP and B3LYP functionals (*a*); first derivatives of XANES spectra, correspondingly (*b*).

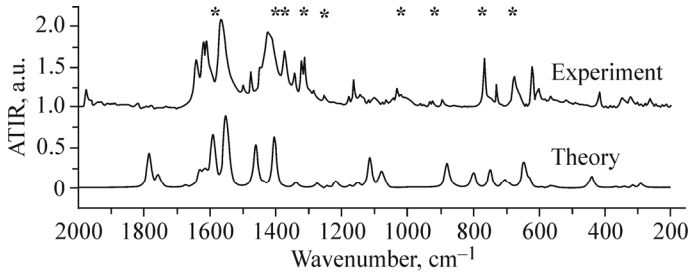

Fig. 4. Comparison between the experimental IR spectrum of $[Cu(O_2CMe)_2(bpy)]$ measured in attenuated total internal reflection mode and the theoretical spectrum. Asterisks mark the data presented in [7].

and B3LYP functionals (shifted for clearness). The positions of the main maximum for the theoretical spectra are well agreed with the experiment. For the XANES spectrum calculated using BP potential, the narrower main maximum with a small shoulder is observed. The indications of the presence of the same shoulder are observed on the experimental spectrum. The *s* and *p* states of copper contribute to the shoulder at the energy 8992 eV. The XANES spectrum calculated using B3LYP potential has the broader main maximum with an additional pre-edge feature at the energy 8988 eV, with this pre-edge peculiarity lacking in the experimental spectrum. Fig. 3*b* presents the first derivatives of the spectra, which allow us to estimate the features of the spectral profiles in detail. The curve shape for the experimental XANES spectrum is the smoothest in comparison to the experimental ones that is partially caused by the experimental conditions. The general view of the first derivative profile for BP spectrum is closest to the experimental one, whereas the derivative for B3LYP has the more distorted view because of the pre-edge feature presence.

Fig. 4 shows the experimental IR spectrum in the so-called finger print region to the far IR region. Stars mark the several peak positions of the IR spectrum, which described in [7]. The full analysis of the available peaks is beyond the scope of this work; however, some comments will be presented. The pair of the strong bands are observed at 1567 cm^{-1} and 1420 cm^{-1} frequencies, which contain stretch vibrations of carboxylate groups from acetate with participation of bond stretches C–C, C=C and C=N in bipyridine. The bands standing by at higher frequencies are supposedly the stretches in the plane of the bipyridine ring exhibiting hypsochromic shift, with the shift being characteristic for similar metal complexes. The other distinctive pair of the bands at 767 cm^{-1} and 730 cm^{-1} frequencies can be assigned to out-of-plane deformation C–H vibrations. Cu-ligand vibrations are usually lie at the frequency lower than 500 cm^{-1} where the group of the medium intensity at 419 cm^{-1} can be attributed to an in-phase stretch of the Cu–O bond.

The model of $[Cu(O_2CMe)_2(bpy)]$ complex consists of 35 atoms and has 99 normal modes of fundamental vibrations. Its frequencies were calculated in the ground state and decreased in scale by coefficient 1.25 for the better agreement with the experiment. The convolution procedure of the calculated intensities with Lorentzian of 20 cm^{-1} width was

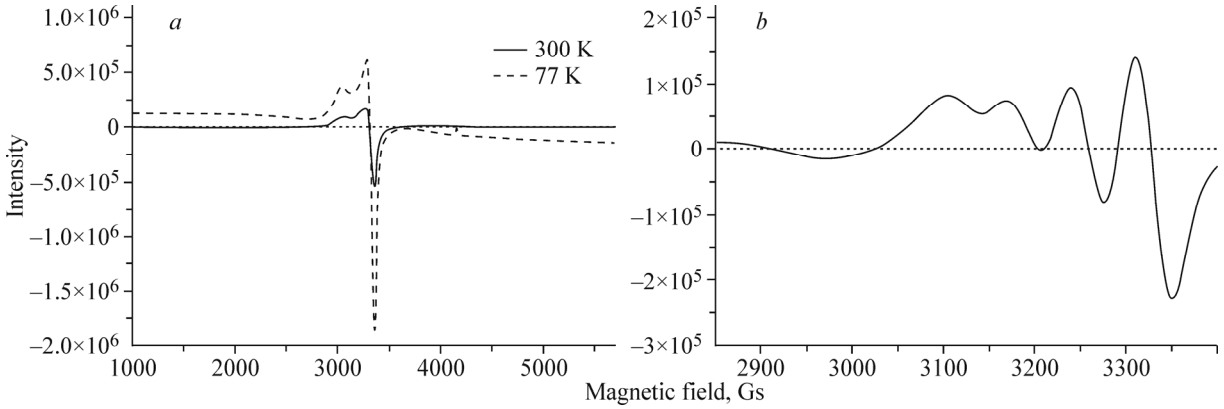

Fig. 5. ESR spectra of $[Cu(O_2CMe)_2(bpy)]$ in solid state at 300 K and 77 K (*a*), and in DMF solution at 300 K (*b*).

performed to compensate the influence of the experimental resolution, the presence of structural defects and thermal effects. The obtained theoretical IR spectrum in Fig. 4 indicates that the main spectroscopic peculiarities of the spectrum well agrees with experimental ones.

Fig. 5 presents ESR spectra of $[Cu(O_2CMe)_2(bpy)]$ complex measured in solid state at temperatures 300 K and 77 K (Fig. 5*a*) and also in DMF solution at 300 K (Fig. 5*b*). The values of the two characteristic parameters *g* and *A* were obtained. The parameter *g* gives information on the geometry of the complex and the tensor *A* is the characteristics of a nucleus-electron hyperfine interaction. The obtained values of *g* and *A* for the Cu(II) acetate-bipyridine complex in DMF solution (Fig. 5*b*) equal to 2.138 G and 69.65 G, correspondingly. These values are typical for Cu(II) mononuclear complexes with a square-planar configuration [43, 44].

CONCLUSIONS

The mononuclear Cu(II) acetate-bipyridine complex with a square-planar geometry was synthesized for the application as a precursor of copper oxide nanoparticles. The theoretical analysis of the X-ray absorption spectra was performed to obtain information on the coordination of the copper center and the electronic configuration. A set of parameters for the DFT modelling was performed on the basis of the comparison of the modelled IR and XANES spectra with experimental data. The model structures of $[Cu(O_2CMe)_2(bpy)]$ complex in aqua and ethanol solutions have been proposed using density functional theory.

This study was financially supported by the Russian Science Foundation (Grant 14-35-00051).

The measurement of X-ray diffraction was performed at the Joint Research Center “Diagnostics of structure and properties of nanomaterials” of Belgorod National Research University. We acknowledge P. A. Knyazev from Institute of Physical and Organic Chemistry (Southern Federal University) for ESR measurements and comments of the obtained results.

REFERENCES

1. R. A. Leising, J. Kim, M. A. Perez, et al., *J. Am. Chem. Soc*., **115**, 9524 (1993).
2. T. R. Felthouse, *Inorg. Chem*., 73 (2007).
3. S. P. Perlepes, S. Paschalidou, J. C. Huffman, et al., *Polyhedron*, No. 14, 1073 (1995).
4. F. P. W. Agterberg, H. A. J. P. Kluit, W. L. Driessen, et al., *Inorg. Chem*., **36**, 4321 (1997).
5. R. A. Reynolds, W. O. Yu, W. R. Dunham, et al., *Inorg. Chem*., **35**, 2721 (1996).
6. B. Ye, X. M. Chen, F. Xue, et al., *Inorg. Chim. Acta*, **299**, No. 1, 1-8 (2000).
7. B. K. Koo, *Bull. Korean Chem. Soc*., **22**, 113 (2011).
8. G. V. Seguel, B. L. Rivas, and P. Órdenes, *J. Chil. Chem. Soc*., **60**, 3080 (2015).
9. M. Hazra, T. Dolai, A. Pandey, et al., *Bioinorg. Chem. Appl*., 1-13 (2014).
10. R. Gomathi, A. Ram, et al., *J. Innovat. Res. Sci. Eng. Technol*., **2**, 4852 (2013).
11. M. A. Oladipo, O. O. Abidemi, and A. D. Olubunmi, *J. Chem. Pharm. Res*., **5**, 69 (2013).
12. S. Y. Ebrahimipour, I. Sheikhshoaie, J. Castro, et al., *Inorg. Chim. Acta*, **430**, 245 (2015).
13. X. Luo, C. Li, D. Yang, et al., *Mater. Chem. Phys*., **151**, 252 (2015).
14. A. B. Devi, D. S. Moirangthem, N. C. Talukdar, et al., *Chin. Chem. Lett*., No. 25, 1615 (2014).
15. L. A. Saghatforoush, R. Mehdizadeh, F. Chalabian, et al., *J. Chem. Pharm. Res*., **3**, 691 (2011).
16. M. Atanasov, P. Comba, B. Martin, et al., *J. Comput. Chem*., **27**, 1263 (2006).
17. G. F. Caramori, R. L. T. Parreira, and A. M. D. C. Ferreira, *Int. J. Quantum Chem*., **112**, 625 (2012).
18. S. Y. Ebrahimipour, I. Sheikhshoaie, M. Mohamadi, et al., *Spectrochim. Acta A*, **142**, 410 (2015).
19. C. Fliedel, V. Rosa, C. I. M. Santos, et al., *Dalton Trans*., **43**, 13041 (2014).
20. S. Kababya, J. Nelson, C. Calle, et al., *J. Am. Chem. Soc*., **128**, 2017 (2006).
21. X. Lu, C.-M. L. Wu, S. Wei, et al., *J. Phys. Chem. A*, **114**, 1178 (2010).

22. H. Zhang, B. Yao, L. Zhao, et al., *J. Am. Chem. Soc*., **136**, 6326 (2014).
23. J. P. Perdew, *Phys. Rev. B*, **34**, 7406 (1986).
24. P. J. Stephens, F. J. Devlin, C. F. Chabalowski, et al., *J. Phys. Chem*., **98**, 11623 (1994).
25. A. D. Becke, *J. Chem. Phys*., **98**, 5648 (1993).
26. A. Sengul, H. Agac, B. Coban, et al., *Turk. J. Chem*., **35**, 25 (2011).
27. D. Karakaş and K. Sayın, *Ind. J. Chem. A*, **52**, 480 (2013).
28. R. Kumar, S. Obrai, J. Mitra, et al., *Spectrochim. Acta. A*, **115**, 244 (2013).
29. Z. D. Matovic, A. Meetsma, V. D. Miletic, et al., *Inorg. Chim. Acta*, **360**, 2420 (2007).
30. N. Novoa, F. Justaud, P. Hamon, et al., *Polyhedron*, **86**, 81 (2015).
31. K. A. Lomachenko, C. Garino, E. Gallo, et al., *Phys. Chem. Chem. Phys*., **15**, 16152 (2013).
32. G. te Velde, F. M. Bickelhaupt, E. J. Baerends, et al., *J. Comput. Chem*., **22**, 931 (2001).
33. C. F. Guerra, J. Snijders, G. te Velde, et al., *Theor. Chem. Acc*., **99**, 391 (1998).
34. *ADF2014*, SCM, Theoretical Chemistry, Vrije Universiteit, Netherlands (2014).
35. A. Bérces, R. M. Dickson, L. Fan, et al., *Comput. Phys. Commun*., **100**, 247 (1997).
36. H. Jacobsen, A. Bérces, D. P. Swerhone, et al., *Comput. Phys. Commun*., **100**, 263 (1997).
37. S. K. Wolff, *Int. J. Quantum Chem*., **104**, 645 (2005).
38. J. P. Perdew, K. Burke, and M. Ernzerhof, *Phys. Rev. Lett*., **77**, 3865 (1996).
39. O. Bunău and Y. Joly, *J. Phys.: Condens. Matter*, **21**, 345501 (2009).
40. S. A. Guda, A. A. Guda, M. A. Soldatov, et al., *J. Chem. Theor. Comput*., **11**, 4512 (2015).
41. H. O. Omoregie, N. Obi-Egbedi, and J. Woods, *Int. J. Chem*., **6**, 71 (2014).
42. L. Herrag, B. Hammouti, S. Elkadiri, et al., *Corros. Sci*., **52**, 3042 (2010).
43. M. G. Savelieff, T. D. Wilson, Y. Elias, et al., *Proc. Natl. Acad. Sci. USA*, **105**, 7919 (2008).
44. B. Kozlevcar and P. Šegedin, *Croat. Chem. Acta*, **81**, 369 (2008).